Stochastic finite element response analysis using random eigenfunction expansion

S E Pryse[1] and S Adhikari[1]

[1] *Zienkiewicz Centre for Computational Engineering, College of Engineering, Swansea University, Swansea SA1 8EN, UK*

Abstract

A mathematical form for the response of the stochastic finite element analysis of elliptical partial differential equations has been established through summing products of random scalars and random vectors. The method is based upon the eigendecomposition of a system's stiffness matrix. The computational reduction is achieved by only summing the dominant terms and by approximating the random eigenvalues and the random eigenvectors. An error analysis has been conducted to investigate the effect of the truncation and the approximations. Consequently, a novel error minimisation technique has been applied through the Galerkin error minimisation approach. This has been implemented by utilising the orthogonal nature of the random eigenvectors. The proposed method is used to solve three numerical examples: the bending of a stochastic beam, the flow through a porous media with stochastic permeability and the bending of a stochastic plate. The results obtained through the proposed random eigenfunction expansion approach are compared with those obtained by using direct Monte Carlo Simulations and by using polynomial chaos.

Keywords: Stochastic differential equations; eigenfunctions; Galerkin; finite element; eigendecomposition; spectral decomposition; reduced methods.

1 Introduction

Uncertainties can substantially affect the analysis of physical structures. These uncertainties can occur in the properties of the material, in the geometry or boundary conditions of the structure or in the applied loads [1]. In order to represent the uncertainties that occur in physical systems, a stochastic finite element method [SFEM] can be applied. This method has been applied to numerous problems including structural mechanics, fluid mechanics and heat

transfer problems. Both static [2, 3] and dynamic [4, 5] scenarios can be represented through this method. In this work, a stochastic elliptic partial differential equation is considered

$$-\nabla^n[a(x,\omega)\nabla^n u(x,\omega)] = p(x) \qquad x \text{ in } \mathcal{D} \tag{1}$$

with the associated Dirichlet condition

$$u(x,\omega) = 0; \qquad x \text{ on } \mathcal{D} \tag{2}$$

In Equation (1), u refers to the governing variable and ∇ refers to the differential operator (for a single dimensional problem $\nabla = \frac{\partial}{\partial x}$) and $n = 1, 2$. The value of n would depend on the physical problem under consideration. When dealing with a flow through a porous media n would be equal to 1, and for the bending of a beam or a plate n would be equal to 2. Both scenarios are discussed in this paper. The spatial dimension under consideration is a bounded domain $\mathcal{D} \in \mathbb{R}^d$ with piecewise Lipschitz boundary $\partial\mathcal{D}$ where d is less than four. $(\Omega, \mathcal{F}, \mathcal{D})$ is a probability space where $\omega \in \Omega$ is a sample point from the sampling space Ω, $\mathcal{F}$ is the complete σ-algebra over the subsets of Ω and P is the probability measure. In Equation (1) $a : \mathbb{R}^d \times \Omega \to \mathbb{R}$ is a random field [6], which can be viewed as a set of random variables indexed by $x \in \mathbb{R}^d$. We assume the random field $a(x, \omega)$ to be stationary, square integrable and non-negative. Following the discretization of Equation (1) through the SFEM [7], this work aims to produce a new solution approach through the use of random eigenfuncation.

Direct Monte Carlo Simulation [MCS] has been widely used in collaboration with the SFEM [8]. Although this is a relatively simple method, using a large number of realisations in conjunction with high dimensional matrices can make this method computationally expensive. Numerous approaches have been proposed in order to reduce the computational time. Multi-level Monte Carlo is one such method where the variance of the Monte Carlo estimator is reduced [9, 10, 11]. Other accelerating methods include centroidal Voronoi tessellations [12, 13], Latin hypercube sampling [14] and quasi Monte Carlo [15, 16]. In spite of the high computational cost linked with the direct MCS method, the error and the computational cost associated with other methods are regularly compared with the direct MCS method [17, 18].

Other methods are available to calculate functional statistics which avoids the use of computationally expensive sampling methods. One such approach is the perturbation method [19, 20, 21]. In such an approach, a Taylor series expansion is used to approximate the structural response. By assuming that the Taylor series converges, the greater the number of terms kept in the series, the higher the accuracy of the response [22]; however publications using an order greater than two are uncommon due to high computational cost. A considerable disadvantage is that the coefficients of variation can't exceed 15% of the mean value of the variable under consideration [8]. Other approaches include Neumann expansions [23, 24, 25] and linear algebra techniques [26]. The stochastic Galerkin method is also popular [27, 28]. This method projects the response on an orthogonal basis that spans the stochastic space.

Another class of methods which have been widely used are spectral methods. This class originates from Wiener's work [29] where the homogeneous chaos method is initially defined. One of the first applications of the chaos expansion for stochastic finite elements is contained in [7]. If the random variables are deemed Gaussian, a polynomial chaos approach can be considered. This approach has been widely used to model different physical scenarios including structural [7], flow [30] and heat transfer [31] problems. However, due to the high computational cost of large systems, numerous reduction methods have been suggested. These include [32] where a spectral decomposition of the deterministic matrix is performed, and only the dominant eigenvalues and eigenvectors retained. [33] have designed an optimisation algorithm which makes the polynomial chaos approximation computationally feasible. Other spectral methods include the Wiener-Askey chaos expansion [34, 35] and the reduced basis method [36, 37].

In Section 2 an overview of the spectral stochastic finite element method is presented. The random eigenfunction approach is proposed in Section 3, whilst Section 4 discusses different ways of approximating random eigenvalues and eigenvectors. Section 5 includes a novel error analysis which is followed by a novel error minimising technique. The new approach is applied to a stochastic Euler-Bernoulli beam, a flow through a stochastic porous media and to the stochastic mechanics of a bending elastic plate in Section 6 and the major conclusions are presented in Section 7.

2 Discretization of the stochastic PDE

The random process $a(x,\omega)$ seen in Equation (1) can be expanded by a generalised Fourier expansion known as the Karhunen-Loève expansion

$$a(x,\omega) = a_0(x) + \sum_{i=1}^{\infty} \sqrt{\tilde{\lambda}_i}\widetilde{\xi}_i(\omega)\tilde{\boldsymbol{\phi}}_i(x) \tag{3}$$

Here a_0 is the mean function and $\tilde{\lambda}_i$ and $\tilde{\boldsymbol{\phi}}_i(x)$ are the eigenvalues and eigenvectors that satisfy the integral equation

$$\int_D C_a(x_1,x_2)\tilde{\boldsymbol{\phi}}_j(x_1)\,dx_1 = \tilde{\lambda}_j\tilde{\boldsymbol{\phi}}_j(x_2) \qquad \forall\, j = 1,2,... \tag{4}$$

where $C_a(x_1,x_2)$ is the covariance function. The $\widetilde{\xi}_i(\omega)$ seen in the Karhunen-Loève expansion corresponds to random variables. If the random process is deemed Gaussian, $\widetilde{\xi}_i(\omega)$ would be standard Gaussian random variables. For other types of random processes, the random variables may possess other distribution types. After truncating the series seen in Equation (3) to the Mth term, the resulting equation can be substituted into the original stochastic elliptical partial differential equation. By applying appropriate boundary conditions, the

discretized equation takes the form

$$\left[\mathbf{A}_0 + \sum_{i=1}^{M} \xi_i(\omega)\mathbf{A}_i\right] \mathbf{u}(\omega) = \mathbf{f} \tag{5}$$

where $\mathbf{A}_0 \in \mathbb{R}^{n\times n}$ represents a deterministic, positive definite, symmetric matrix. $\mathbf{A}_i \in \mathbb{R}^{n\times n}$ are general symmetric matrices for $i = 1, 2, ...M$, $\mathbf{u}(\omega) \in \mathbb{R}^n$ the response vector and $\mathbf{f} \in \mathbb{R}^n$ the deterministic input force vector. The details of obtaining the discretized equivalent of Equation (1) have been omitted, but can be located in numerous textbooks including [7]. The method proposed in this paper is general in nature, therefore the random variables seen in Equation (5) are not restricted to any specific distribution.

3 Random eigenfunction expansion

3.1 Motivation behind the proposed approach

For simplicity, we express Equation (5) as

$$\mathbf{A}(\omega)\mathbf{u}(\omega) = \mathbf{f} \tag{6}$$

where the random matrix $\mathbf{A}(\omega) = \mathbf{A}_0 + \sum_{i=1}^{M} \xi_i(\omega)\mathbf{A}_i$. The matrix $\mathbf{A}(\omega)$ can be considered as a random stiffness matrix. As the system under consideration is static, a mass matrix is not required. We will consider problems where the value of M and the number of degrees of freedom in a system are sufficiently large. For small values of M computational reduction can be achieved. However when M is sufficiently large the solution of Equation (6) poses computational challenges.

The exact solution to the set of stochastic linear equations given above can be obtained through direct MCS. Convergence is guaranteed if the number of realisations is sufficiently large and all realisations of $\mathbf{A}(\omega)$ are positive definite. However, direct MCS can be seen as a computationally expensive method [38], especially if there is a large number of stochastic linear equations to be solved. In order to avoid the use of direct MCS, alternative methods have been explored. The response of Equation (6) can be represented through summing products of random scalars and deterministic vectors

$$\mathbf{u}(\omega) = \sum_{j=1}^{M_1} a_j(\omega)\mathbf{g}_j \tag{7}$$

where $a_j(\omega) \in \mathbb{R}$ and $\mathbf{g}_j \in \mathbb{R}^n$ represent the random scalars and deterministic vectors respectively. M_1 corresponds to the number of terms in the summation. Equation (7) can be considered as the polynomial chaos method

$$\mathbf{u}(\omega) = \sum_{k=1}^{P} H_k(\xi(\omega))\mathbf{u}_k \tag{8}$$

where $H_k(\xi(\omega))$ represents the polynomial chaoses (corresponding to the random scalars), and $\mathbf{u}_k$ represents unknown deterministic vectors that need to be determined. The value of P is determined by a basic random variable M and by the order of the Polynomial Chaos expansion p. In this instance, M corresponds to the order of the Karhunen-Loève expansion. The value of P is determined by the following expression

$$P = \sum_{j=0}^{p} \frac{(M+j-1)!}{j!(M-1)!} \tag{9}$$

It is evident that P increases rapidly when either the order of the Karhunen-Loève expansion or the order of the Polynomial Chaos expansion is increased. The unknown vector $\mathbf{u}_k$ can be obtained by using a Galerkin error minimising approach [7]. This approach leads to a system of linear equations of size $nP \times nP$. A possible drawback to this approach is the high computational cost if either n or P is large.

Another possibility is acquiring a solution that is of a similar form to Equation (7) where both the scalars and vectors are deemed random

$$\mathbf{u}(\omega) = \sum_{j=1}^{M_2} a_j(\omega)\mathbf{g}_j(\omega) \tag{10}$$

where $a_j(\omega) \in \mathbb{R}$ and $\mathbf{g}_j(\omega) \in \mathbb{R}^n$ represent the random scalars and vectors respectively. M_2 corresponds to the number of terms in the summation. Due to the vector terms in Equation (7) being deterministic, only Equation (10) can incorporate the full stochastic nature of Equation (6). The aim of this paper is to obtain an expression for the response of Equation (6) that is of the same form as Equation (10).

3.2 Derivation of the response vector

The random eigenvalue problem is initially considered

$$\mathbf{A}(\omega)\boldsymbol{\phi}_k(\omega) = \lambda_k(\omega)\boldsymbol{\phi}_k(\omega); \quad k = 1, 2, \ldots n \tag{11}$$

For convenience, the matrices of the random eigenvalues and eigenvectors of $\mathbf{A}(\omega)$ are defined as follows

$$\begin{aligned} \boldsymbol{\Lambda}(\omega) &= \operatorname{diag}\left[\lambda_1(\omega), \lambda_2(\omega), \ldots, \lambda_n(\omega)\right] \in \mathbb{R}^{n\times n} \quad \text{and} \\ \boldsymbol{\Phi}(\omega) &= \left[\boldsymbol{\phi}_1(\omega), \boldsymbol{\phi}_2(\omega), \ldots, \boldsymbol{\phi}_n(\omega)\right] \in \mathbb{R}^{n\times n} \end{aligned} \tag{12}$$

The random eigenvalues are arranged in ascending order so $\lambda_1(\omega) < \lambda_2(\omega) < \ldots < \lambda_n(\omega)$ and the corresponding eigenvectors are arranged in the same order. Due to the orthogonal property of $\boldsymbol{\Phi}(\omega)$ it is apparent that $\boldsymbol{\Phi}(\omega)^{-1} = \boldsymbol{\Phi}(\omega)^T$. Thus the following identities can be defined (ω has been omitted for notational convenience)

$$\boldsymbol{\Phi}^T\mathbf{A}\boldsymbol{\Phi} = \boldsymbol{\Lambda}; \quad \mathbf{A} = \boldsymbol{\Phi}^{-T}\boldsymbol{\Lambda}\boldsymbol{\Phi}^{-1} \quad \text{and} \quad \mathbf{A}^{-1} = \boldsymbol{\Phi}\boldsymbol{\Lambda}^{-1}\boldsymbol{\Phi}^T \tag{13}$$

Using these identities, the response of Equation (6) can be expressed as

$$\mathbf{u}(\omega) = \mathbf{A}(\omega)^{-1}\mathbf{f} \tag{14}$$

or

$$\mathbf{u}(\omega) = \mathbf{\Phi}\mathbf{\Lambda}^{-1}\mathbf{\Phi}^T\mathbf{f} = \sum_{j=1}^{n} \underbrace{\frac{\boldsymbol{\phi}_j^T(\omega)\mathbf{f}}{\lambda_j(\omega)}}_{a_j(\omega)} \underbrace{\boldsymbol{\phi}_j(\omega)}_{g_j(\omega)} \tag{15}$$

Equation (15) is of the same form as Equation (10) where $\frac{\boldsymbol{\phi}_j^T(\omega)\mathbf{f}}{\lambda_j(\omega)}$ corresponds to the scalar term $a_j(\omega)$, $\boldsymbol{\phi}_j(\omega)$ corresponds to the vector term $\mathbf{g}_j(\omega)$ and n corresponds to M_2. In this particular method, $\boldsymbol{\phi}_j(\omega)$ forms a complete orthogonal basis. Therefore, it can be concluded that the response of Equation (6) can be expressed in the same form as Equation (10).

However, calculating the exact values of $a_j(\omega)$ and $\mathbf{g}_j(\omega)$ could prove difficult, and this could consequently take longer than directly solving Equation (14). This has motivated a new reduced approach which would give an efficient and accurate representation of the response. The computational cost of evaluating Equation (15) can be improved in two ways. The number of terms in the summation could be reduced or $a_j(\omega)$ and $\mathbf{g}_j(\omega)$ could be evaluated efficiently by suitable approximations.

The series given in (15) could be truncated after a certain amount of terms. The higher order terms of the summation have a relatively low value due to the eigenvalues being ordered ascendingly; this allows the low valued terms to be discarded whilst retaining the dominant terms in the series. The number of terms retained in Equation (15) can either be predefined or determined by

$$\frac{\lambda_{1_0}}{\lambda_{t_0}} > \epsilon_{trunc} \tag{16}$$

where λ_{1_0} corresponds to the first, and therefore the smallest deterministic eigenvalue. λ_{t_0} corresponds to the largest deterministic eigenvalue that satisfies the above inequality. The value of t would correspond to the number of terms kept in the truncation. The deterministic eigenvalues arising in the inequality can be computed from the corresponding deterministic system and the value of ϵ_{trunc} is to be selected appropriately. Hence Equation (15) can be truncated as follows

$$\mathbf{u}(\omega) \approx \sum_{j=1}^{t} \frac{\boldsymbol{\phi}_j^T(\omega)\mathbf{f}}{\lambda_j(\omega)}\boldsymbol{\phi}_j(\omega) \tag{17}$$

where $\lambda_j(\omega)$ and $\boldsymbol{\phi}_j(\omega)$ represent the random eigenvalues and the random eigenvectors and $t < n \ll nP$. The full response for $\mathbf{u}(\omega)$ can be obtained by performing a MCS on each sample.

4 Approximating the random eigensolutions

Approximating the random eigenvalues and eigenvectors may also improve the calculation cost and there are numerous methods of doing so. Direct MCS can by used in collaboration with the random eigenvalue problem in order to calculate the exact values of the random eigenvalues and eigenvectors; however this method is computationally expensive. Numerous papers have proposed improvements to the direct MCS method. Ref. [39] uses a subspace iteration scheme with carefully selected start-vectors, whilst [40] compares the subspace iteration method with an approach that uses component mode synthesis. [41] proposes a method of obtaining the random eigenvalues and random eigenvectors through expanding the random eigenvalues and eigenvectors by a polynomial chaos approach. However this method is computationally expensive. Due to its low computational cost, a first-order perturbation approach for obtaining the random eigenvalues and eigenvectors has been explored.

Solutions of different perturbation methods are obtained by truncating the Taylor series expansion. Due to its efficiency and ease, the first-order perturbation method has been used. The jth random eigenvalue and its corresponding random eigenvector is given by

$$\lambda_j \approx \lambda_{j_0} + \sum_{k=1}^{M} \left(\frac{\partial \lambda_j}{\partial \xi_k} \right) \xi_k(\omega) \tag{18}$$

$$\text{and} \quad \boldsymbol{\phi}_j \approx \boldsymbol{\phi}_{j_0} + \sum_{k=1}^{M} \left(\frac{\partial \boldsymbol{\phi}_j}{\partial \xi_k} \right) \xi_k(\omega) \tag{19}$$

where λ_{j_0} and $\boldsymbol{\phi}_{j_0}$ are the jth deterministic eigenvalue and eigenvector and $\xi_k(\omega)$ represents a set of Gaussian random variables with mean zero and unit variance. By differentiating the eigenvalue equation with respect to ξ_k, pre-multiplying with $\boldsymbol{\phi}^T$ and utilising that $\boldsymbol{\phi}_{j_0}^T \boldsymbol{\phi}_{j_0} = 1$, $\frac{\partial \lambda}{\partial \xi_k}$ can be expressed as

$$\frac{\partial \lambda_j}{\partial \xi_k} = \boldsymbol{\phi}_{j_0}^T \frac{\partial \mathbf{A}}{\partial \xi_k} \boldsymbol{\phi}_{j_0} \tag{20}$$

In the instance of Equation (20), $\frac{\partial \mathbf{A}}{\partial \xi_k} = \mathbf{A}_k$.

The derivative of $\boldsymbol{\phi}_j$ with respect to ξ_k can be calculated by expanding $\frac{\partial \boldsymbol{\phi}_j}{\partial \xi_k}$ as a linear combination of the deterministic eigenvalues and eigenvectors [42, 43]

$$\frac{\partial \boldsymbol{\phi}_j}{\partial \xi_k} = \sum_{i=1 \neq j}^{N} \alpha_{jki} \boldsymbol{\phi}_i \quad \text{where} \quad \alpha_{jki} = \frac{\boldsymbol{\phi}_{i_0}^T \frac{\partial \mathbf{A}}{\partial \xi_k} \boldsymbol{\phi}_{j_0}}{\lambda_{j_0} - \lambda_{i_0}} \tag{21}$$

For completeness it can be noted that $\alpha_{jki} \boldsymbol{\phi}_i = 0$ when $i = j$. In the instance of the above equation, $\frac{\partial \mathbf{A}}{\partial \xi_k} = \mathbf{A}_k$. This method requires all the deterministic eigenvalues and eigenvectors to be known. A simplified approach is proposed in [44] where only a limited number of eigenvalues and eigenvectors are needed.

For the case of repeated eigenvalues, the general method of approximating the response of Equation (6) continues to be valid. However a different approach would be needed whilst approximating the eigenvectors to that given in this section. This case is beyond the scope of this paper.

Other approaches based on the perturbation method have been proposed to approximate random eigensolutions. An approach based on the perturbation method and the Rayleigh quotient is presented in [45]; this method results in an improvement in the accuracy of the eigensolution. However [46] reports that the accuracy of the approximations obtained by the first-order perturbation method and the method presented in [45] deteriorates if the uncertainty in the system is sufficiently large. Ref. [46] proposes numerous methods to overcome this problem. One way of doing so is by implementing a Padé approximation which is seen in [47].

5 Error minimisation and analysis

5.1 Error analysis

The error associated with the random eigenfunction expansion method can be defined in numerous ways. The solution vector obtained through the random eigenfunction expansion method can be directly compared with the true solution, or the solution obtained through the random eigenfunction expansion can be reintroduced into Equation (6). Initially, the error vector arising from a single realisation has been defined by comparing the solution vectors of the random eigenfunction expansion and the direct MCS method

$$\epsilon_\alpha = \mathbf{u}_{\text{REFE}} - \mathbf{u}_{\text{MCS}} \tag{22}$$

where $\mathbf{u}_{\text{REFE}} \in \mathbb{R}^n$ denotes the solution vector obtained through the random eigenfunction expansion method and $\mathbf{u}_{\text{MCS}} \in \mathbb{R}^n$ the solution vector obtained through the direct MCS method. The mean squared error [MSE] arising from the proposed method can be derived from the trace of the covariance matrix. By taking all the realisations needed to execute the random eigenfunction expansion and the direct MCS methods into account, the MSE can be expressed as

$$\mathbb{MSE}\{\epsilon_\alpha\} = \mathbb{E}\Big\{ \text{Trace}\Big\{ \big[\mathbf{u}_{\text{REFE}} - \mathbf{u}_{\text{MCS}}\big] \big[\mathbf{u}_{\text{REFE}} - \mathbf{u}_{\text{MCS}}\big]^T \Big\} \Big\} \tag{23}$$

The errors arising due to the truncation of Equation (17), and due to the approximation of the eigenvalues and eigenvectors are discussed separately.

5.1.1 Error arising from the truncation

We initially consider the case of Equation (17) being truncated to give only the first t terms. We assume that the exact values of the eigenvalues and eigenvectors are know for each realisation. For each realisation, the full random eigenvalue

and eigenvector matrices can be partitioned as follows

$$\boldsymbol{\Lambda}(\omega) = [\boldsymbol{\Lambda}_b(\omega)|\boldsymbol{\Lambda}_c(\omega)] \quad \text{and} \quad \boldsymbol{\Phi}(\omega) = [\boldsymbol{\Phi}_b(\omega)|\boldsymbol{\Phi}_c(\omega)] \tag{24}$$

where $\boldsymbol{\Lambda}_b(\omega) \in \mathbb{R}^{t\times t}$ and $\boldsymbol{\Phi}_b(\omega) \in \mathbb{R}^{n\times t}$ denote the blocks that include the random eigenvalues and eigenvectors that are used in the proposed method. $\boldsymbol{\Lambda}_c(\omega) \in \mathbb{R}^{(n-t)\times(n-t)}$ and $\boldsymbol{\Phi}_c(\omega) \in \mathbb{R}^{n\times(n-t)}$ denote the blocks that include the unused random eigenvalues and eigenvectors. For notational convenience, (ω) has been omitted for the remainder of this sub-section. By using the relationship given in Equation (15) and the partitions given in Equation (24), the exact response of a single realisation can take the following form

$$\begin{aligned}
\mathbf{u} &= [\boldsymbol{\Phi}\boldsymbol{\Lambda}^{-1}\boldsymbol{\Phi}^T]\mathbf{f} \\
&= \big([\boldsymbol{\Phi}_b|\boldsymbol{\Phi}_c][\boldsymbol{\Lambda}_b|\boldsymbol{\Lambda}_c]^{-1}[\boldsymbol{\Phi}_b|\boldsymbol{\Phi}_c]^T]\big)\mathbf{f} \\
&= \underbrace{\Big[\boldsymbol{\Phi}_b\boldsymbol{\Lambda}_b^{-1}\boldsymbol{\Phi}_b^T\Big]\mathbf{f}}_{\beta} + \underbrace{\Big[\boldsymbol{\Phi}_c\boldsymbol{\Lambda}_c^{-1}\boldsymbol{\Phi}_c^T\Big]\mathbf{f}}_{\gamma}
\end{aligned} \tag{25}$$

β corresponds to the response when Equation (17) is truncated to include the initial t terms. Therefore, the error arising due to the truncation can be contributed to γ. The error of a single realisation can be given by

$$\epsilon_\gamma = \big[\boldsymbol{\Phi}_c\boldsymbol{\Lambda}_c^{-1}\boldsymbol{\Phi}_c^T\big]\mathbf{f} \tag{26}$$

By taking into account the realisations needed to calculate the random eigenvalues and eigenvectors, the expected mean squared error can be expressed as

$$\begin{aligned}
\mathbb{MSE}\{\epsilon_\gamma\} &= \mathbb{E}\Bigg\{\text{Trace}\Bigg\{\Big(\big[\boldsymbol{\Phi}_c\boldsymbol{\Lambda}_c^{-1}\boldsymbol{\Phi}_c^T\big]\mathbf{f}\Big)\Big(\big[\boldsymbol{\Phi}_c\boldsymbol{\Lambda}_c^{-1}\boldsymbol{\Phi}_c^T\big]\mathbf{f}\Big)^T\Bigg\}\Bigg\} \\
&= \mathbb{E}\Bigg\{\text{Trace}\Big\{\boldsymbol{\Phi}_c\boldsymbol{\Lambda}_c^{-1}\boldsymbol{\Phi}_c^T\mathbf{f}\mathbf{f}^T\boldsymbol{\Phi}_c\boldsymbol{\Lambda}_c^{-1}\boldsymbol{\Phi}_c^T\Big\}\Bigg\}
\end{aligned} \tag{27}$$

Due to the cyclic nature of traces [48], and due to $\boldsymbol{\Phi}_c^T\boldsymbol{\Phi}_c$ being equal to the identity matrix, the above expression can be simplified

$$\mathbb{MSE}\{\epsilon_\gamma\} = \mathbb{E}\Bigg\{\text{Trace}\Big\{\boldsymbol{\Lambda}_c^{-2}\boldsymbol{\Phi}_c^T\mathbf{f}\mathbf{f}^T\boldsymbol{\Phi}_c\Big\}\Bigg\} \tag{28}$$

The error arising from the truncation of Equation (17) will be small if the unused eigenvalues are significantly large. However, as finding the expected value is a linear operator, the $\boldsymbol{\Lambda}_c^{-2}$ term introduces an extra degree of difficulty. This may be overcome by expanding $\boldsymbol{\Lambda}_c$ by the perturbation method. Due to the sparse nature of $\boldsymbol{\Lambda}_c$, its inverse can be expressed as

$$\boldsymbol{\Lambda}_c^{-1} = \begin{bmatrix}
\frac{1}{\lambda_{t+1}} & 0 & \cdots & 0 & 0 \\
0 & \frac{1}{\lambda_{t+2}} & \cdots & 0 & 0 \\
\vdots & \vdots & \ddots & \vdots & \vdots \\
0 & 0 & \cdots & \frac{1}{\lambda_{n-1}} & 0 \\
0 & 0 & \cdots & 0 & \frac{1}{\lambda_n}
\end{bmatrix} \tag{29}$$

By applying the perturbation method, $\mathbf{\Lambda}_c^{-1}$ can be expressed as

$$\mathbf{\Lambda}_c^{-1} = \mathbf{\Lambda}_{c_0}^{-1} + \Delta_c \tag{30}$$

where $\mathbf{\Lambda}_{c_0}^{-1}$ is the inverses of the deterministic eigenvalues of block c and Δ_c a matrix that captures the random nature of the eigenvalues. The square of Equation (30) is given by

$$\begin{aligned} \mathbf{\Lambda}_c^{-2} &= (\mathbf{\Lambda}_{c_0}^{-1} + \Delta_c)(\mathbf{\Lambda}_{c_0}^{-1} + \Delta_c) \\ &= \mathbf{\Lambda}_{c_0}^{-2} + 2\mathbf{\Lambda}_{c_0}^{-1}\Delta_c + \Delta_c^2 \end{aligned} \tag{31}$$

If the eigenvalues are significantly large and the coefficients of variation not excessively large, Δ_c^2 will be small. Consequently, Equation (31) can be approximated by

$$\mathbf{\Lambda}_c^{-2} \approx \mathbf{\Lambda}_{c_0}^{-2} + 2\mathbf{\Lambda}_{c_0}^{-1}\Delta_c \tag{32}$$

Therefore Equation (28) can be approximated by

$$\begin{aligned} \mathbb{MSE}\{\epsilon_\gamma\} &\approx \mathbb{E}\Bigg\{ \text{Trace}\Big\{ \{\mathbf{\Lambda}_{c_0}^{-2} + 2\mathbf{\Lambda}_{c_0}^{-1}\Delta_c\}\mathbf{\Phi}_c^T\mathbf{f}\mathbf{f}^T\mathbf{\Phi}_c \Big\} \Bigg\} \\ &= \text{Trace}\Big\{ \mathbf{\Lambda}_{c_0}^{-2}\mathbb{E}\Big\{ \mathbf{\Phi}_c^T\mathbf{f}\mathbf{f}^T\mathbf{\Phi}_c \Big\} + 2\mathbf{\Lambda}_{c_0}^{-1}\mathbb{E}\Big\{ \Delta_c\mathbf{\Phi}_c^T\mathbf{f}\mathbf{f}^T\mathbf{\Phi}_c \Big\} \Big\} \end{aligned} \tag{33}$$

where the expected values arising in the above equation can be calculated through applying a MCS. It is apparent that identifying the dominant term in Equation (33) depends on the characteristics of the governing discrete equation. As the eigenvalues incorporated in Λ_c are generally large, it can be easily deduced that $\mathbf{\Lambda}_{c_0}^{-2} < \mathbf{\Lambda}_{c_0}^{-1}$. Under the assumption of small randomness it can also be deduced that $\mathbb{E}\Big\{ \mathbf{\Phi}_c^T\mathbf{f}\mathbf{f}^T\mathbf{\Phi}_c \Big\} > \mathbb{E}\Big\{ \Delta_c\mathbf{\Phi}_c^T\mathbf{f}\mathbf{f}^T\mathbf{\Phi}_c \Big\}$ due to the small nature of Δ_c. Therefore to determine the dominant term, the relationships between $\mathbf{\Lambda}_{c_0}^{-2}$ and $\mathbb{E}\Big\{ \Delta_c\mathbf{\Phi}_c^T\mathbf{f}\mathbf{f}^T\mathbf{\Phi}_c \Big\}$, and between $2\mathbf{\Lambda}_{c_0}^{-1}$ and $\mathbb{E}\Big\{ \mathbf{\Phi}_c^T\mathbf{f}\mathbf{f}^T\mathbf{\Phi}_c \Big\}$ are important to consider. Therefore Equation (33) gives an intuitive account of the factors which contribute towards the error induced by the truncation. However if all the eigenvalues and eigenvectors are retained in the original summation, the expected mean squared error arising due to the truncation would naturally equate to zero.

5.1.2 Error arising from approximating the random eigenvalues and eigenvectors

As calculating the exact random eigenvalues and eigenvectors through solving the random eigenvalue problem is computationally expensive, approximating these values can be beneficial. However approximating the random eigenvalues and eigenvectors can lead to an increased error. Whilst investigating the error arising from approximating the eigenvalues and eigenvectors, Equation (17)

has not been truncated. The error arising when approximating the random eigenvalues and eigenvectors of a single realisation is given by

$$\epsilon_\delta = \left[\left(\mathbf{\Phi}_r \mathbf{\Lambda}_r^{-1} \mathbf{\Phi}_r^T\right)\mathbf{f} - \left(\mathbf{\Phi}_t \mathbf{\Lambda}_t^{-1} \mathbf{\Phi}_t^T\right)\mathbf{f}\right] \tag{34}$$

where $\mathbf{\Lambda}_r \in \mathbb{R}^{n\times n}$ and $\mathbf{\Phi}_r \in \mathbb{R}^{n\times n}$ denote the approximated random eigenvalues and eigenvectors and $\mathbf{\Lambda}_t \in \mathbb{R}^{n\times n}$ and $\mathbf{\Phi}_t \in \mathbb{R}^{n\times n}$ denote the exact values of the random eigenvalues and eigenvectors obtained by solving the random eigenvalue problem. By taking into account the realisations needed to calculate the random eigenvalues and eigenvectors, the expected mean squared error can be expressed as

$$\begin{aligned}
\mathbb{MSE}\{\epsilon_\delta\} &= \mathbb{E}\Big\{ \mathrm{Trace}\Big\{ \left[\left(\mathbf{\Phi}_r \mathbf{\Lambda}_r^{-1} \mathbf{\Phi}_r^T\right)\mathbf{f} - \left(\mathbf{\Phi}_t \mathbf{\Lambda}_t^{-1} \mathbf{\Phi}_t^T\right)\mathbf{f}\right] \left[\left(\mathbf{\Phi}_r \mathbf{\Lambda}_r^{-1} \mathbf{\Phi}_r^T\right)\mathbf{f} - \left(\mathbf{\Phi}_t \mathbf{\Lambda}_t^{-1} \mathbf{\Phi}_t^T\right)\mathbf{f}\right]^T \Big\} \Big\} \\
&= \mathbb{E}\Big\{ \mathrm{Trace}\Big\{ \mathbf{\Phi}_r \mathbf{\Lambda}_r^{-1} \mathbf{\Phi}_r^T \mathbf{f}\mathbf{f}^T \mathbf{\Phi}_r \mathbf{\Lambda}_r^{-1} \mathbf{\Phi}_r^T - \mathbf{\Phi}_r \mathbf{\Lambda}_r^{-1} \mathbf{\Phi}_r^T \mathbf{f}\mathbf{f}^T \mathbf{\Phi}_t \mathbf{\Lambda}_t^{-1} \mathbf{\Phi}_t^T \\
&\qquad - \mathbf{\Phi}_t \mathbf{\Lambda}_t^{-1} \mathbf{\Phi}_t^T \mathbf{f}\mathbf{f}^T \mathbf{\Phi}_r \mathbf{\Lambda}_r^{-1} \mathbf{\Phi}_r^T + \mathbf{\Phi}_t \mathbf{\Lambda}_t^{-1} \mathbf{\Phi}_t^T \mathbf{f}\mathbf{f}^T \mathbf{\Phi}_t \mathbf{\Lambda}_t^{-1} \mathbf{\Phi}_t^T \Big\} \Big\}
\end{aligned} \tag{35}$$

This expression can be simplified due to the cyclic nature of traces. It can be noted that $\mathbf{\Phi}_t^T \mathbf{\Phi}_t$ is equal to the identity matrix. However as $\mathbf{\Phi}_r$ refers to the matrix containing the approximated eigenvectors, $\mathbf{\Phi}_r^T \mathbf{\Phi}_r$ is not exactly equal to the identity matrix. As the value of product of $\mathbf{\Phi}_r^T$ and $\mathbf{\Phi}_r$ is extremely close to the identity matrix, for the reminder of this section we will approximate $\mathbf{\Phi}_r^T \mathbf{\Phi}_r$ by the identity matrix. The following equation has used this approximation, however if $\mathbf{\Phi}_r^T \mathbf{\Phi}_r$ were to be re-introduced into the equation, the accuracy of the MSE would improve

$$\begin{aligned}
\mathbb{MSE}\{\epsilon_\delta\} \approx \mathrm{Trace}\Big\{ \mathbb{E}\Big\{ &\mathbf{\Lambda}_r^{-2} \mathbf{\Phi}_r^T \mathbf{f}\mathbf{f}^T \mathbf{\Phi}_r - \mathbf{\Phi}_r \mathbf{\Lambda}_r^{-1} \mathbf{\Phi}_r^T \mathbf{f}\mathbf{f}^T \mathbf{\Phi}_t \mathbf{\Lambda}_t^{-1} \mathbf{\Phi}_t^T \\
&- \mathbf{\Phi}_t \mathbf{\Lambda}_t^{-1} \mathbf{\Phi}_t^T \mathbf{f}\mathbf{f}^T \mathbf{\Phi}_r \mathbf{\Lambda}_r^{-1} \mathbf{\Phi}_r^T + \mathbf{\Lambda}_t^{-2} \mathbf{\Phi}_t^T \mathbf{f}\mathbf{f}^T \mathbf{\Phi}_t \Big\} \Big\}
\end{aligned} \tag{36}$$

Similarly to the case seen in Equation (33), the $\mathbf{\Lambda}_r^{-2}$, $\mathbf{\Lambda}_t^{-2}$, $\mathbf{\Lambda}_r^{-1}$ and $\mathbf{\Lambda}_t^{-1}$ terms arising in Equation (36) can be approximated by a perturbation method. However introducing all the additional perturbation terms does not necessarily improve the intuitive understanding. The expected values arising in Equation (36) can be computed by applying a MCS for each sample.

The formulae seen thus far in this section could be applied, for example, to compare the effect of keeping additional terms in the truncation. The mean squared error could be computed for t and $t+1$ terms in order to identify the effect of discarding the additional term. However the formulae are predominantly given to gain an insight into the nature of the error. As the time needed to compute the expectation operators arising in Equations (33) and (36) is high, computing the errors for practical problems may not be feasible. This

has motivated further discussion in order to lower the errors without the need of explicitly computing the expectation values given in this section. Consequently a technique has been suggested to lower the error through utilising a Galerkin approach.

5.2 Error minimisation using the Galerkin approach

In Sections 3.2 and 4, through utilising approximations for the random eigenvalues and eigenvectors and by truncating Equation (17), an expression for the response of Equation (6) has been derived. The approximation of the random eigenvalues and eigenvectors, in addition to the truncations has motivated an error minimising technique. Thus we are proposing a variant of the approximation proposed in Equation (17) by introducing an error minimisation technique. In order to implement this, the error vector arising from a single realisation of the random eigenfunction expansion method has been defined as

$$\epsilon_\zeta(\omega) = \mathbf{A}(\omega)\mathbf{u}(\omega) - \mathbf{f} \tag{37}$$

where $\mathbf{u}(\omega)$ represents the solution vector obtained with Equation (17). A Galerkin approach is proposed where the error is made orthogonal to the random eigenvectors. For this new approach, the solution vector has been modified to take the following form

$$\widetilde{\mathbf{u}}(\omega) = \sum_{j=1}^{t} \left(\frac{\boldsymbol{\phi}_j^T(\omega)\mathbf{f}}{\lambda_j(\omega)} + c_j \right) \boldsymbol{\phi}_j(\omega) \tag{38}$$

where $\lambda_j \in \mathbb{R}$ and $\boldsymbol{\phi}_j \in \mathbb{R}^n$ represent the random eigenvalues and eigenvectors, $\mathbf{f} \in \mathbb{R}^n$ the deterministic applied force and $c_j \in \mathbb{R}$ are unknown constants to be determined. The error vector is now given by

$$\widetilde{\epsilon_\zeta}(\omega) = \mathbf{A}(\omega)\widetilde{\mathbf{u}}(\omega) - \mathbf{f} \tag{39}$$

The unknown constants c_j can be obtained through using a Galerkin approach where the error is made orthogonal to the random eigenvectors

$$< \boldsymbol{\phi}_k(\omega), \widetilde{\epsilon}_\zeta(\omega) >= 0 \quad \forall \quad k = 1, 2, ...t \tag{40}$$

where $< \mathbf{u}, \mathbf{v} >= \mathbb{E}\{\mathbf{u}^T\mathbf{v}\}$ is the inner product. By using this condition and the expression for $\widetilde{\epsilon}_\zeta(\omega)$ obtained in Equation (39), one has

$$\mathbb{E}\left\{ \boldsymbol{\phi}_k^T \left[\mathbf{A} \left[\sum_{j=1}^{t} \left(\frac{\boldsymbol{\phi}_j^T\mathbf{f}}{\lambda_j} + c_j \right) \boldsymbol{\phi}_j \right] - \mathbf{f} \right] \right\} = 0$$
$$\forall \quad j = 1, 2, ...t \quad \text{and} \quad k = 1, 2, ...t \tag{41}$$

where $\mathbb{E}\{\bullet\}$ denotes the expected value. For notational convenience, (ω) has been omitted. It can be shown that the unknown coefficients arising in Equation

(41) can be expressed in a closed-form

$$\mathbb{E}\left\{\sum_{j=1}^{t}\left(\boldsymbol{\phi}_k^T\mathbf{A}\boldsymbol{\phi}_j\right)\left(\frac{\boldsymbol{\phi}_j^T\mathbf{f}}{\lambda_j}\right)+\sum_{j=1}^{t}\left(\boldsymbol{\phi}_k^T\mathbf{A}\boldsymbol{\phi}_j\right)c_j-\boldsymbol{\phi}_k^T\mathbf{f}\right\}=0$$
$$\forall \quad j=1,2,...t \quad \text{and} \quad k=1,2,...t \quad (42)$$

$$\mathbb{E}\left\{\sum_{j=1}^{t}\left(\boldsymbol{\phi}_k^T\mathbf{A}\boldsymbol{\phi}_j\right)c_j\right\}=\mathbb{E}\left\{\boldsymbol{\phi}_k^T\mathbf{f}\right\}-\mathbb{E}\left\{\sum_{j=1}^{t}\left(\boldsymbol{\phi}_k^T\mathbf{A}\boldsymbol{\phi}_j\right)\left(\frac{\boldsymbol{\phi}_j^T\mathbf{f}}{\lambda_j}\right)\right\}$$
$$\forall \quad j=1,2,...t \quad \text{and} \quad k=1,2,...t \quad (43)$$

$$c_k=\left[\mathbb{E}\left\{\sum_{j=1}^{t}\boldsymbol{\phi}_k^T\mathbf{A}\boldsymbol{\phi}_j\right\}\right]^{-1}\left[\mathbb{E}\left\{\boldsymbol{\phi}_k^T\mathbf{f}\right\}-\mathbb{E}\left\{\sum_{j=1}^{t}\frac{(\boldsymbol{\phi}_k^T\mathbf{A}\boldsymbol{\phi}_j)(\boldsymbol{\phi}_k^T\mathbf{f})}{\lambda_j}\right\}\right]$$
$$\forall \quad j=1,2,...t \quad \text{and} \quad k=1,2,...t \quad (44)$$

Equation (44) gives an explicit closed form for the unknown coefficients c_k where $\lambda_j, \boldsymbol{\phi}_j$ and $\boldsymbol{\phi}_k$ correspond to approximated random eigenvalues and eigenvectors. The expected values arising in Equation (44) can be computed by using low-order MCS. Thus by reintroducing the unknown coefficients c_k into Equation (38), one can assume that Equation (38) is a re-analysis of the solution obtained in Equation (17). The error minimisation approach presented is not unique. Rather than appearing as additive factors, the unknown constants could appear as multiplicative factors. If multiplicative factors were to be used, the Galerkin approach would be implemented in a similar manner.

6 Application examples

The Gaussian nature of the random variables is not a pre-requisite for the method proposed in the paper. However for the numerical examples considered here, Gaussian random variables are used to compare the results with the polynomial chaos approach. For each sample it has been ensured that the matrix $\mathbf{A}(\omega)$ is non singular and positive definite. Although numerous cost effective methods for calculating the random eigenvalues and eigenvectors are available, as the aim of this paper is to express a viable solution for Equation (1) in the form of Equation (10), for its efficiency and ease the first-order perturbation method has be used in all examples.

6.1 Euler-Bernoulli beam with stochastic properties

6.1.1 Model

The computational method has been applied to a cantilever beam clamped at one end i.e. the displacement at the clamped end is zero. A deterministic

vertical point load is applied at the free end of the beam, where $P = 1.00$ N. The length of the beam under consideration is 1.00 m, and its cross-section is a rectangle of length 0.03 m and height 0.003 m. Figure 1 illustrates the system.

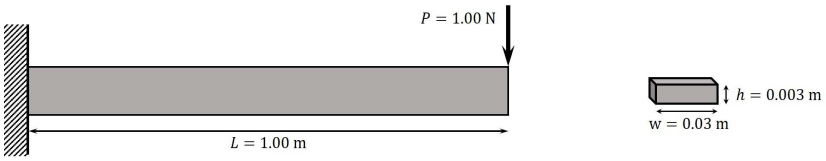

Figure 1: Beam system

The system has been discretized into a 100 elements by using SFEM. Details of the discretization can be found in numerous books such as [49]. Consequently, the dimension of the corresponding determinant matrix is 200×200. For the deterministic case, the Young's modulus is $E = 69 \times 10^9$ Nm^{-2} thus corresponding to an aluminium beam [50]. The deterministic second moment of area (moment of inertia) of the beam is

$$I = \frac{0.03 \times 0.003^3}{12} = 6.75 \times 10^{-11} \text{ m}^4 \tag{45}$$

The bending rigidity of the beam, EI, can be assumed to be a stationary Gaussian random field of the form

$$EI(x, \omega) = \overline{EI}(1 + a(x, \omega)) \tag{46}$$

where $\overline{EI} = 4.66$ Nm^2. The function $a(x, \omega)$ represents a stationary Gaussian field with zero mean, with x being the coordinate direction of the length of the beam. The standard deviation is given by $0.2\overline{EI}$, and the covariance function by

$$C_a(x_1, x_2) = \sigma_a^2 e^{(|x_1 - x_2|)/\mu_a} \tag{47}$$

where μ_a is the correlation length and σ_a the standard deviation. In this instance, the correlation length is set as 1.00 m in order to correspond with the length of the beam. The non-differentiability of the covariance model at the origin does not significantly affect our results due to the displacement at the origin being zero. However if we were to assess the stress at the origin instead of the displacement, the model chosen would need to be reassessed [51]. The Karhunen-Loève expansion of the stiffness matrix, given by Equation (3), has been truncated and two terms have been kept. The solution for the displacement of the beam has been obtained through different methods. The methods being:

- Direct Monte Carlo Simulation applied through directly solving Equation (14) (MCS)
- Random eigenvalue eigenfunction expansion (REFE)

- Random eigenvalue eigenfunction expansion including the Galerkin error minimising method (REFEG)
- Polynomial Chaos of order four (PC)

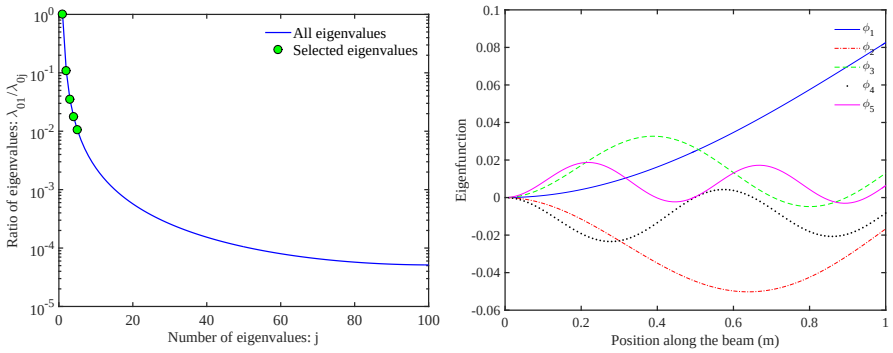

(a) Ratio of eigenvalues

(b) First five eigenvectors

Figure 2: Ratio of eigenvalues and the first five eigenvectors of the beam problem

All the methods have been simulated 10,000 times and the performances of the approximation methods compared with that of the direct MCS approach. For both the REFE and REFEG methods, Equations (17) and (38) have been truncated to include the first 5 terms.

Figure (2) illustrates the ratio between the first and the jth eigenvalue of the deterministic system and the first five eigenvalues have been highlighted. Figure (2) also illustrates the first five eigenvectors of the deterministic system.

6.1.2 Results and error analysis

The displacement of the beam can be normalised by

$$h = \frac{f_0 L^3}{3EI} \tag{48}$$

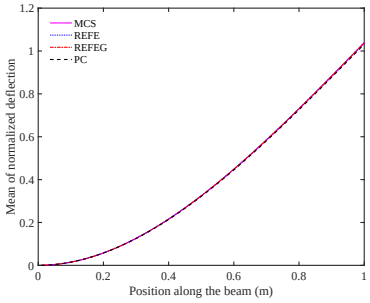

(a) Mean

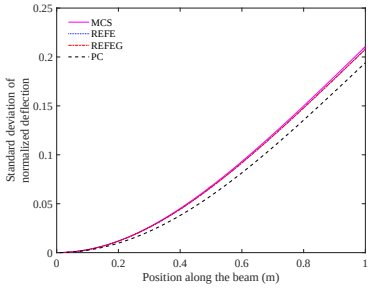

(b) Standard deviation

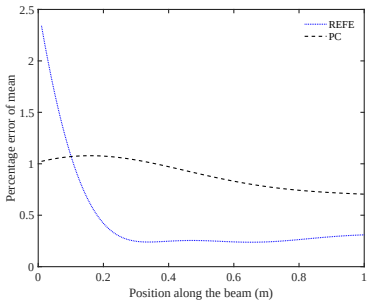

(c) Percentage error of mean

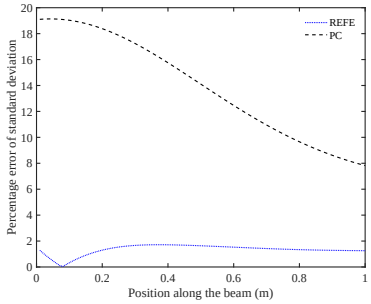

(d) Percentage error of standard deviation

Figure 3: The mean and the standard deviation of the normalised vertical displacement of the beam and a comparison of the percentage error of the mean and the standard deviation of the normalised vertical displacement between the MCS and REFE methods

A detailed reference to this value is give in [52]. This normalisation value ensures that the deterministic vertical displacement has a value of 1 at the tip. Figures (3a) and (3b) illustrate the mean and standard deviation of the normalised vertical displacement at all the nodes of the beam. The percentage error arising when using the REFE and the PC methods in place of the direct MCS is illustrated in Figures (3c) and (3d). The percentage error is represented by

$$\epsilon_{percentage} = 100 * \frac{|FMCS - COMP|}{FMCS} \tag{49}$$

where FMCS indicates the solution of the direct MCS, and COMP the solution

Method	**MCS**	**REFE**	**REFEG**	**PC**
CPU time (sec)	9.59	0.86	4.07	1.07

Table 1: The CPU times for calculating the response of the beam problem by using the MCS, REFE, REFEG and PC methods

of the comparable methods. Barring the initial 0.10 m of the bar, the percentage

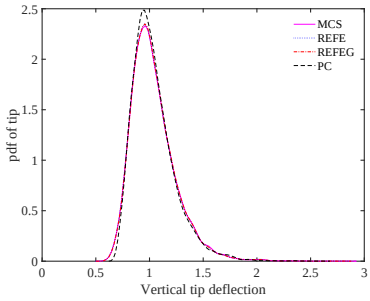

(a) Pdf of the vertical displacement

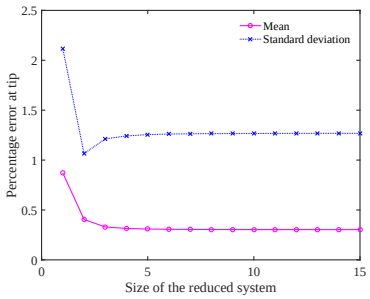

(b) Error of mean and standard deviation - REFE

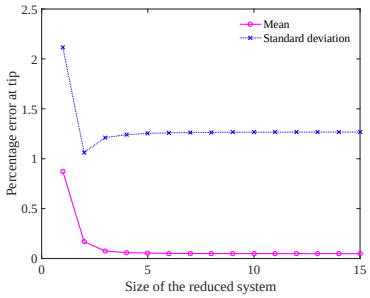

(c) Error of mean and standard deviation - REFEG

Figure 4: The pdf of the vertical displacement at the tip of the beam obtained with the MCS, REFE, REFEG and PC methods. Percentage errors of the mean and the standard deviation of the tip displacement using REFE and REFEG with different truncation values in Equations (17) and (38)

error of the mean and standard deviation of the REFE method is considerably lower than the PC method. Table (1) contains the CPU times for the four methods attempted. The computational cost was calculated on a standard 24 GB RAM computer with a 3.60 GHz processor. The pdf of the vertical displacement at the tip for the MCS, REFE, REFEG and PC methods is illustrated in Figure (4a). The error of the vertical tip displacement when using the REFE and REFEG methods instead of the direct MCS method is shown in Figures (4b) and (4c) for different values of t i.e. the number of terms in Equations (17) and (38). The percentage error of the standard deviation at the tip of the beam is similar for both the REFE and REFEG methods for all truncation values. However a clear, albeit small reduction is seen in the percentage error of the mean when the REFEG method is used instead of the REFE method.

6.2 Flow through a stochastic porous media

6.2.1 Method

In the previous example, the Euler Bernoulli beam was modelled as a one-dimensional object. The porous media in this example has a higher spatial dimension, where the two-dimensional domain is a rectangle of width $W = 0.60$ m and Length $L = 1.00$ m. In this instance, the response measurement is the head of the system. Using the stochastic finite element method, the domain has been divided into an uniform mesh of 60×36 square elements. A constant flux $q = 1$ cm s^{-1} enters the media along its boundary at $y = -0.3$ m and $x \in [0.3, 0.5]$ m. In order to obtain a static state, the head is fixed at $h = 0$ cm along the boundary of the media at $x = -0.5$ m and $y \in [0.17, 0.30]$ m. The coordinate (0.0, 0.0) is located at the centre of the rectangle. The flux has been set to zero along the remaining boundaries. Figure (5) illustrates the configuration.

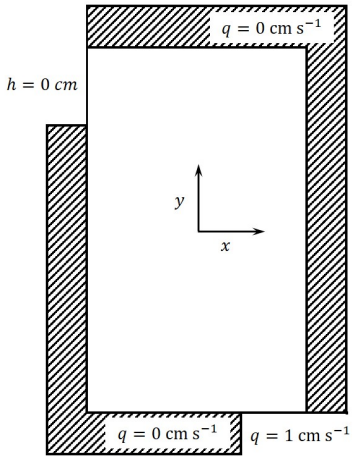

Figure 5: Flow system

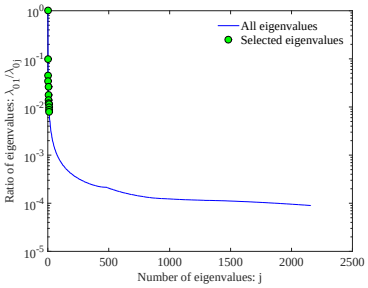

Figure 6: Ratio of eigenvalues for the flow through porous media problem

A Gaussian hydraulic conductivity (k) with a 2D exponential covariance function is considered. In order to obtain the 2D covariance function, two 1D exponential covariance functions have been multiplied together. One has a correlation length of $b_x = L/5$ and depends on x, whilst the other has a correlation length of $b_y = W/5$ and depends on y. In both the 1D exponential covariance functions, two terms of the Karhunen-Loève expansion are kept. Thus the full Karhunen-Loève expression is calculated by summing a deterministic matrix with four random matrices. The mean and standard deviation of the hydraulic conductivity are given by $\overline{k} = 1$ cm s^{-1} and $\sigma = 0.2\overline{k}$. Full details of the finite element method used can be obtained in numerous textbooks including [53].

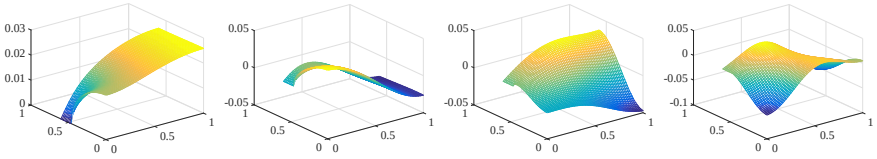

(a) First eigenvector **(b)** Second eigenvector **(c)** Third eigenvector **(d)** Fourth eigenvector

Figure 7: First four eigenvectors of the stiffness matrix for the flow through porous media problem

Similarly to the previous example, the response has been obtained using different methods. The direct Monte Carlo Simulation (MCS) has been applied with 10,000 samples. For both the REFE and REFEG approaches, Equations (17) and (38) have been truncated to include the first 12 terms. Figure (6) shows the ratio between the first and the jth deterministic eigenvalue; the first 12 eigenvalues are highlighted. Figure (7) illustrates the first four eigenvectors of the deterministic system. The PC used is of order four. This implies that 70 polynomials are used whilst expanding the response. Consequently, a linear system of size 71,330 needs to be solved.

6.2.2 Results and error analysis

Figures (8) and (9) are contour plots of the mean and standard deviation of the head for the different methods. The contour plots obtained from the PC method seem to reflect the results obtained by the MCS method slightly better than the contour plots obtained from the REFE and REFEG methods. A considerable portion of the error from REFE and REFEG methods can be asserted to the region close to the entry point of the flux i.e. at $y = -0.3$ m and $x \in [0.3, 0.5]$ m. This is depicted in more detail in Figure (10) where the mean and standard deviation of the percentage error arising from the REFE and REFEG methods are illustrated. Table (2) contains the CPU times for the four methods.

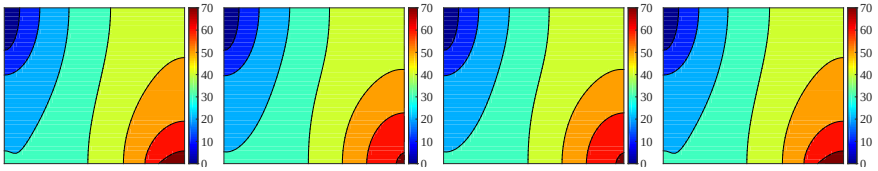

(a) MCS **(b)** REFE **(c)** REFEG **(d)** PC

Figure 8: Contour plots of the mean of the head (cm) obtained with the MCS, REFE, REFEG and PC methods. The x and y axis are respectively the positions in the x direction with $x \in [-0.5, 0.5]$ m and in the y direction with $y \in [-0.3, 0.3]$ m

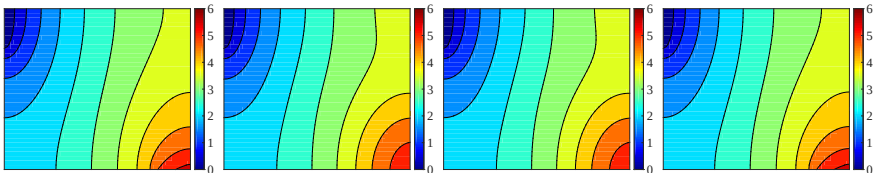

(a) MCS **(b)** REFE **(c)** REFEG **(d)** PC

Figure 9: Contour plots of the standard deviation of the head (cm) obtained with the MCS, REFE, REFEG and PC methods. The x and y axis are respectively the positions in the x direction with $x \in [-0.5, 0.5]$ m and in the y direction with $y \in [-0.3, 0.3]$ m

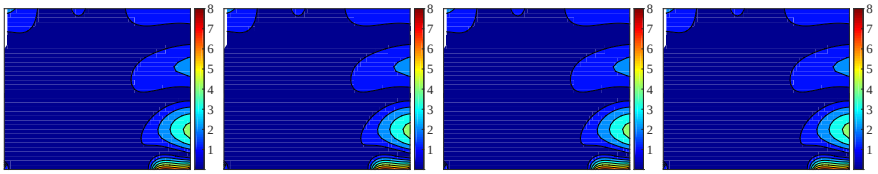

(a) ϵ_p of μ_p (REFE) **(b)** ϵ_p of σ_p (REFE) **(c)** ϵ_p of μ_p (REFEG) **(d)** ϵ_p of σ_p (REFEG)

Figure 10: Contour plots of the percentage error (ϵ_p) of the mean (μ_p) and standard deviation (σ_p) of the REFE and REFEG methods compared to the MCS method. The x and y axis are respectively the positions in the x direction with $x \in [-0.5, 0.5]$ m and in the y direction with $y \in [-0.3, 0.3]$ m

Method	**MCS**	**REFE**	**REFEG**	**PC**
CPU time (sec)	2.06×10^3	13.10	71.71	123.73

Table 2: The CPU times for calculating the response of the flow problem by using the MCS, REFE, REFEG and PC methods

The pdf of the response at coordinates $(0.0, 0.0)$ and $(0.5, -0.2)$ have been

calculated by using the four different methods. The pdfs are plotted in Figure (11). There is no significant difference between the pdfs obtained by the REFE and REFEG methods even though the computational times differ significantly. The mean and standard deviation obtained through the MCS and the random eigenvalue and eigenvector methods are similar at coordinate $(0.0, 0.0)$. The coordinate $(0.5, -0.2)$ corresponds to a pocket of high percentage error for both the mean and standard deviation when using the REFE and REFEG methods. This is seen in Figure (10) and is further exemplified in Figure (11b). In this instance, for both the REFE and REFEG methods, the pdf of the head does not mimic that of the MCS method very well. However if more terms are kept in the truncations, the pdf of the approximation methods will get much closer to that of the MCS method. The total mean squared error [MSE] arising from the REFE and REFEG methods is illustrated in Figure (11c) for different truncation values of Equations (17) and (38). Although a decrease in the MSE is seen as the number of terms in the expansions increase, the introduction of the error minimising approach does not decrease the error significantly.

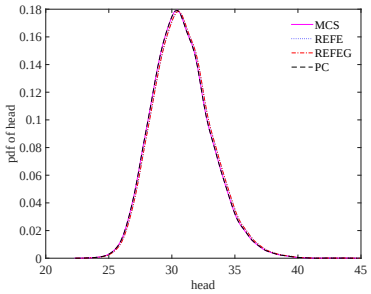

(a) Pdf of the head at $(0.0, 0.0)$

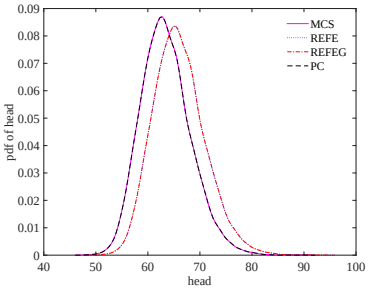

(b) Pdf of the head at $(0.5, -0.2)$

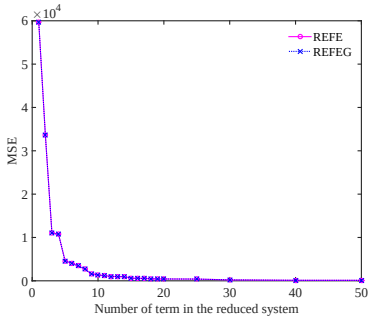

(c) MSE of the whole system

Figure 11: Pdfs of the head (cm) at $(0.0, 0.0)$ and $(0.5, -0.2)$ and the mean square error of the whole system when using REFE and REFEG for different truncation values of Equations (17) and (38).

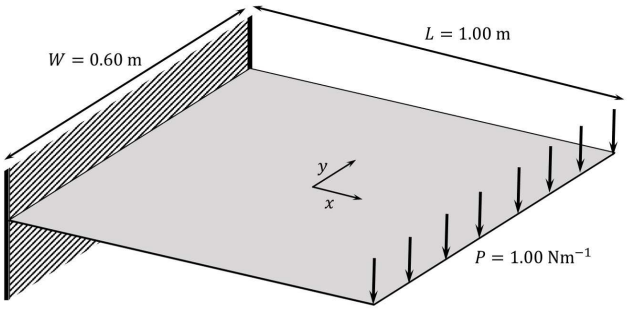

Figure 12: Plate system

6.3 Bending of an elastic plate with stochastic properties

6.3.1 Model

The plate bending problem can often be considered as an extension to the Euler Bernoulli beam scenario [54]. By using the proposed methods, a numerical example of a thin bending plate is given where the underlying equations of the bending plate is governed by the Kirchhoff-Love plate theory. The rectangular plate under consideration has a length (L) of 1.00 m and a width (W) of 0.60 m. As in the previous example, the centre of the plate has coordinates $(0.0, 0.0)$. The plate is clamped along its width ($x = -0.30$ m), and an uniformly distributed deterministic load of value $P = 1.00$ Nm^{-1} is applied at $x = 0.30$ m. Figure (12) illustrates the configuration. By using an uniform mesh, the plate has been divided into 25 elements in the x direction and 15 elements in the y direction. This leads to a deterministic stiffness matrix of dimension 1200. The bending rigidity of the plate, D, can be assumed to be a stationary Gaussian random field of the form

$$D(x, y, \omega) = \overline{D}(1 + a(x, y, \omega)) \tag{50}$$

where $a(x, y, \omega)$ is a stationary Gaussian field with zero mean and x and y represent the coordinate directions of the length and width of the plate. The mean value of D can be expressed by

$$\overline{D} = \frac{Eh^3}{12(1 - \mu^2)} \tag{51}$$

where E is the Young's Modulus, h the thickness of the plate and μ the Poisson's ratio of the plate material. For the given example $E = 200 \times 10^9$ Nm^{-2}, $h = 0.003$ m and $\mu = 0.3$ thus resulting in $\overline{D} = 494.51$ Nm. The values used imply that the plate is made of steel. The standard deviation of D is given by $\sigma = 0.2\overline{D}$. The covariance function for D is obtained by multiplying two 1D exponential covariance functions together; one of the 1D functions has a correlation length of $b_x = L/5$ and depends on x, whilst the other has a correlation length of $b_y = W/5$ and depends on y. Two terms in the Karhunen-Loève

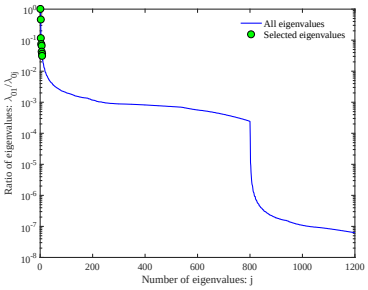

Figure 13: Ratio of eigenvalues for the bending of an elastic plate problem

expansion (see Equation (3)) have been kept in both the 1D functions. Thus the full Karhunen-Loève expression is calculated by summing a deterministic matrix with four random matrices. A detailed account of the finite elements method used can be found in numerous textbooks including [49].

Four different methods have been used to obtain the response of the system: a direct MCS, REFE, REFEG and PC. All methods have used 10,000 samples. For both the random eigenvalue and eigenvector approaches, Equations (17) and (38) have been truncated to include the first 8 terms. Figure (13) shows the ratio between the first and the jth eigenvalue; the first 8 eigenvalues are highlighted. A PC of order four is used, thus a linear system of size 84,000 needs to be solved.

6.3.2 Results and error analysis

Figure (14) contains contour plots of the mean of the vertical displacement of the plate. In a similar manner, Figure (15) contains contour plots of the standard deviation of the vertical displacement. The contour plots of the mean and standard deviation of the vertical displacement obtained by the REFE and REFEG methods mimic those obtained by the MCS method pretty well. Figure (16) contains the contour plots of the percentage error of the mean and standard deviation of the vertical displacement for the REFE and REFEG methods. A higher percentage of error is seen by the clamped end of the plate in both instances. Table (3) contains the CPU times for the four methods; it's apparent that the REFE method is considerably faster than the other methods.

For all methods, the pdfs of the vertical displacement at coordinate (0.26, -0.02) have been calculated and plotted in Figure (17). There is no significant difference between the pdfs of the different methods. Figure (17) also illustrates the mean and standard deviation of the vertical displacement along all nodes of

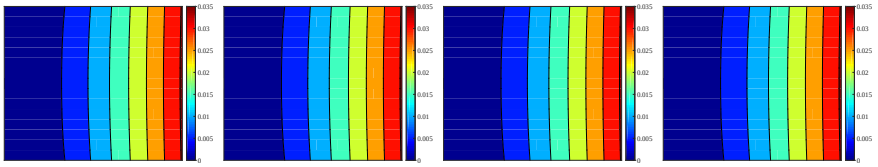

(a) MCS **(b)** REFE **(c)** REFEG **(d)** PC

Figure 14: Contour plots of the mean of the vertical displacement (m) of the plate when applying the MCS, REFE, REFEG and PC methods. The x and y axis are respectively the positions in the x direction with $x \in [-0.5, 0.5]$ m and in the y direction with $y \in [-0.3, 0.3]$ m

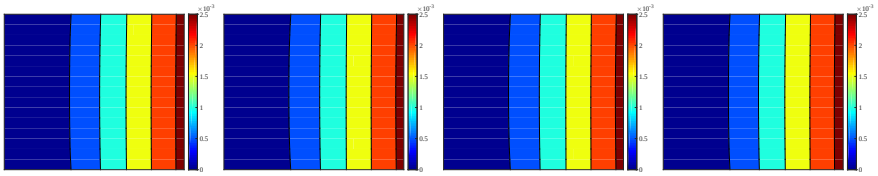

(a) MCS **(b)** REFE **(c)** REFEG **(d)** PC

Figure 15: Contour plots of the standard deviation of the vertical displacement (m) of the plate when applying the MCS, REFE, REFEG and PC methods. The x and y axis are respectively the positions in the x direction with $x \in [-0.5, 0.5]$ m and in the y direction with $y \in [-0.3, 0.3]$ m

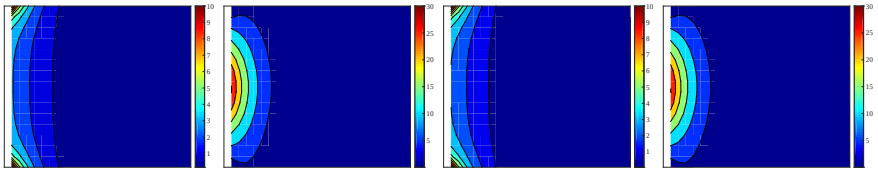

(a) ϵ_p of μ_p (REFE) **(b)** ϵ_p of σ_p (REFE) **(c)** ϵ_p of μ_p (REFEG) **(d)** ϵ_p of σ_p (REFEG)

Figure 16: Contour plots of the percentage error (ϵ_p) of the mean and standard deviation of the REFE and REFEG methods compared to the MCS method. The x and y axis are respectively the positions in the x direction with $x \in [-0.5, 0.5]$ m and in the y direction with $y \in [-0.3, 0.3]$ m

Method	**MCS**	**REFE**	**REFEG**	**PC**
CPU time (sec)	3.75×10^3	4.04	44.36	146.03

Table 3: The CPU times for calculating the response of the bending plate problem by using the MCS, REFE, REFEG and PC methods

the plate at $y = -0.02$ m.

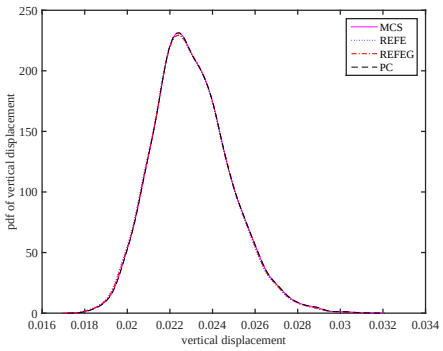

(a) Pdf of the vertical displacement at (0.26,-0.02)

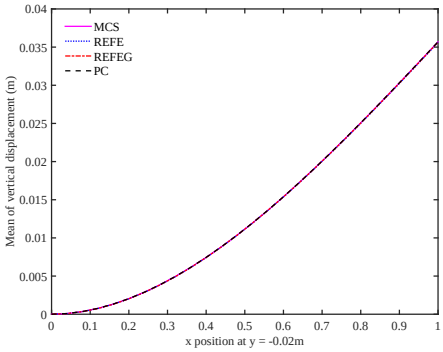

(b) Percentage error of mean along $y = -0.02$ m

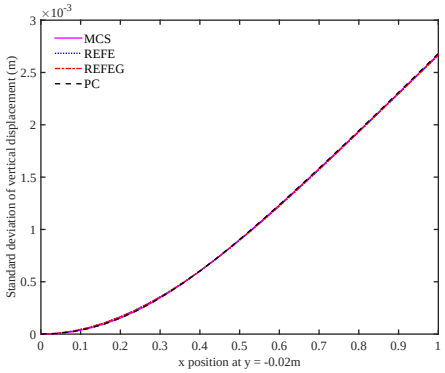

(c) Percentage error of standard deviation along $y = -0.02$ m

Figure 17: The pdf of the vertical displacement of the plate at position (0.26,-0.02) obtained when using the MCS, REFE, REFEG and PC methods. The mean and the standard deviation of the vertical displacement along $y = -0.02$ m is also depicted.

7 Summary and conclusion

7.1 Summary

- It has been established that the mathematical form of the exact solution of discretized stochastic equations must be in the form of $\mathbf{u}(\omega) = \sum_{j=1}^{M_2} a_j(\omega)\mathbf{g}_j(\omega)$, where $a_j(\omega)$ are random scalars and $\mathbf{g}_j(\omega)$ are random vectors and $M_2 = n$ is the dimension of the problem.
- A random eigenfunction approach has been established in order to calculate $a_j(\omega)$ and $\mathbf{g}_j(\omega)$.
- Through approximating and truncating, the computational time of the random eigenfunction approach has been reduced.

- The error arising due to the approximation and truncation has been addressed by using a Galerkin approach.
- A closed-form expression for the unknown coefficients arising due to the Galerkin approach has been obtained by exploiting the orthogonality properties of the random eigenfunctions.
- In comparison to direct Monte Carlo Simulations, the new approach produces accurate results in a faster computational time.

7.2 Conclusion

An approach has been suggested to calculate the response of discretized stochastic elliptic partial differential equations. Through utilising the stochastic finite element method and the random eigenvalue problem, it has been proven that the solution can be represented by summing products of random scalars and random vectors. Due to the high computational cost associated with calculating the exact solution, a reduced approach is proposed where random eigenvalues and eigenvectors are approximated and low valued terms are discarded from the summation. An error analysis has been conducted to analyse the effect of the truncation and the effect of the approximations. A novel Galerkin error minimisation approach is presented where the solution is projected onto random eigenvectors. Consequently, the unknown constants are expressed in an explicit closed form. Due to the nature of the proposed approach, the random variables associated with the method are not confined to a particular distribution.

The proposed method has been used to solve three stochastic elliptic problems (1) the bending of a Euler-Bernoulli cantilever beam, (2) the flow through a porous media, and (3) the bending of an elastic plate. The three systems considered here are characterised by respective stochastic field properties. The proposed method has been applied twice, once with and once without the error minimisation technique. The solutions obtained through the proposed methods have then been compared with those obtained through direct MCS and through the polynomial chaos method. The random variables used in the applications were Gaussian for the purpose of comparative studies. The solutions obtained through the proposed methods are similar to those obtained through direct MCS, however, localised errors are sometimes present if the truncation of the proposed method is too severe. Although the Galerkin error minimisation approach slightly lowers the error, the computational time is significantly longer than when the Galerkin error minimisation approach is not used. The computational time of the proposed method is significantly lower than the corresponding times obtained from the direct MCS and polynomial chaos approaches, especially if the dimension of the discretized system is significantly large. Further work to be carried out would focus on efficient ways of computing random eigenfunctions and performing the model-order reduction.

8 Acknowledgements

The authors acknowledge the financial support received from Engineering Research Network Wales (one of three Sêr Cymru National Research Networks) with Grant No. NRN 125.

References

[1] G. Maymon, Structural Dynamics and Probabilistic Analysis for Engineers, Butterworth-Heinemann, 2008.

[2] A. Lal, B. N. Singh, R. Kumar, Static response of laminated composite plates resting on elastic foundation with uncertain system properties, Journal of Reinforced Plastics and Composites 26 (8) (2007) 807–829.

[3] B. Z. Xia, D. J. Yu, J. Liu, Transformed perturbation stochastic finite element method for static response analysis of stochastic structures, Finite Elements in Analysis and Design 79 (2014) 9–21.

[4] S. Adhikari, T. Murmu, M. A. McCarthy, Dynamic finite element analysis of axially vibrating nonlocal rods, Finite Elements in Analysis and Design 63 (2013) 42–50.

[5] C. Soize, Stochastic modeling of uncertainties in computational structural dynamics-recent theoretical advances, Journal of Sound and Vibration 332 (10) (2013) 2379–2395.

[6] E. VanMarcke, Random Fields: Analysis and Synthesis, MIT Press, Cambridge MA, 1983.

[7] R. G. Ghanem, P. D. Spanos, Stochastic Finite Elements: A Spectral Approach (revised edition), Dover Publications Inc., 2012.

[8] J. E. Hurtado, A. H. Barbat, Monte carlo techniques in computational stochastic mechanics, Archives of Computational Methods in Engineering 5 (1) (1998) 3–29.

[9] A. Barth, C. Schwab, N. Zollinger, Multi-level monte carlo finite element method for elliptic pdes with stochastic coefficients, Numerische Mathematik 119 (1) (2011) 123–161.

[10] A. Barth, A. Lang, C. Schwab, Multilevel monte carlo method for parabolic stochastic partial differential equations, Bit Numerical Mathematics 53 (1) (2013) 3–27.

[11] J. Charrier, R. Scheichl, A. L. Teckentrup, Finite element error analysis of elliptic pdes with random coefficients and its application to multilevel monte carlo methods, Siam Journal on Numerical Analysis 51 (1) (2013) 322–352.

[12] V. J. Romero, J. V. Burkardt, M. D. Gunzburger, J. S. Peterson, Initial evaluation of Centroidal Voronoi Tessellation method for statistical sampling and function integration, Isuma 2003: Fourth International Symposium on Uncertainty Modeling and Analysis, IEEE, 2003.

[13] V. J. Romero, J. V. Burkardt, M. D. Gunzburger, J. S. Peterson, Comparison of pure and "latinized" centroidal voronoi tessellation against various other statistical sampling methods, Reliability Engineering & System Safety 91 (10-11) (2006) 1266–1280.

[14] J. C. Helton, F. J. Davis, Latin hypercube sampling and the propagation of uncertainty in analyses of complex systems, Reliability Engineering & System Safety 81 (1) (2003) 23–69.

[15] I. G. Graham, F. Y. Kuo, J. A. Nichols, R. Scheichl, C. Schwab, I. H. Sloan, Quasi-monte carlo finite element methods for elliptic pdes with lognormal random coefficients, Numerische Mathematik 131 (2) (2015) 329–368.

[16] F. Y. Kuo, C. Schwab, I. H. Sloan, Quasi-monte carlo finite element methods for a class of elliptic partial differential equations with random coefficients, Siam Journal on Numerical Analysis 50 (6) (2012) 3351–3374.

[17] G. R. Liu, W. Zeng, H. Nguyen-Xuan, Generalized stochastic cell-based smoothed finite element method for solid mechanics, Finite Elements in Analysis and Design 63 (2013) 51–61.

[18] G. Stavroulakis, D. G. Giovanis, M. Papadrakakis, V. Papadopoulos, A new perspective on the solution of uncertainty quantification and reliability analysis of large-scale problems, Computer Methods in Applied Mechanics and Engineering 276 (2014) 627–658.

[19] O. Cavdar, A. Bayraktar, A. Cavdar, S. Adanur, Perturbation based stochastic finite element analysis of the structural systems with composite sections under earthquake forces, Steel and Composite Structures 8 (2) (2008) 129–144.

[20] S. Sakata, F. Ashida, K. Ohsumimoto, Stochastic homogenization analysis of a porous material with the perturbation method considering a microscopic geometrical random variation, International Journal of Mechanical Sciences 77 (2013) 145–154.

[21] L. H. Yao, P. P. He, S. K. Song, A perturbation stochastic finite-element method for groundwater flow models based on an undetermined-coefficients approach, Hydrogeology Journal 18 (7) (2010) 1603–1609.

[22] J. D. Arregui-Mena, L. Margetts, P. M. Mummery, Practical application of the stochastic finite element method, Archives of Computational Methods in Engineering 23 (1) (2016) 171–190.

[23] F. Yamazaki, M. Shinozuka, G. Dasgupta, Neumann expansion for stochastic finite-element analysis, Journal of Engineering Mechanics-Asce 114 (8) (1988) 1335–1354.

[24] Z. Lei, C. Qiu, Neumann dynamic stochastic finite element method of vibration for structures with stochastic parameters to random excitation, Computers & Structures 77 (6) (2000) 651–657.

[25] X. Y. Wang, S. Cen, C. F. Li, Generalized neumann expansion and its application in stochastic finite element methods, Mathematical Problems in Engineering (2013) 1–13.

[26] C. F. Li, Y. T. Feng, D. R. J. Owen, Explicit solution to the stochastic system of linear algebraic equations $(\alpha_1\mathbf{A}_1 + \alpha_2\mathbf{A}_2 \cdots + \alpha_m\mathbf{A}_m)\mathbf{x} = \mathbf{b}$, Computer Methods in Applied Mechanics and Engineering 195 (44-47) (2006) 6560–6576.

[27] I. Babuska, F. Nobile, R. Tempone, A stochastic collocation method for elliptic partial differential equations with random input data, Siam Journal on Numerical Analysis 45 (3) (2007) 1005–1034.

[28] H. G. Matthies, A. Keese, Galerkin methods for linear and nonlinear elliptic stochastic partial differential equations, Computer Methods in Applied Mechanics and Engineering 194 (12-16) (2005) 1295–1331.

[29] N. Wiener, The homogeneous chaos, American Journal of Mathematics 60 (4) (1938) 897–936.

[30] H. N. Najm, Uncertainty quantification and polynomial chaos techniques in computational fluid dynamics, Annual Review of Fluid Mechanics 41 (2009) 35–52.

[31] A. F. Emery, Solving stochastic heat transfer problems, Engineering Analysis with Boundary Elements 28 (3) (2004) 279–291.

[32] B. Pascual, S. Adhikari, A reduced polynomial chaos expansion method for the stochastic finite element analysis, Sadhana-Academy Proceedings in Engineering Sciences 37 (3) (2012) 319–340.

[33] S. Zein, B. Colson, F. Glineur, An efficient sampling method for regression-based polynomial chaos expansion, Communications in Computational Physics 13 (4) (2013) 1173–1188.

[34] D. B. Xiu, G. E. Karniadakis, The wiener-askey polynomial chaos for stochastic differential equations, Siam Journal on Scientific Computing 24 (2) (2002) 619–644.

[35] D. B. Xiu, G. E. Karniadakis, Modeling uncertainty in flow simulations via generalized polynomial chaos, Journal of Computational Physics 187 (1) (2003) 137–167.

[36] P. Chen, A. Quarteroni, G. Rozza, Comparison between reduced basis and stochastic collocation methods for elliptic problems, Journal of Scientific Computing 59 (1) (2014) 187–216.

[37] S. K. Sachdeva, P. B. Nair, A. J. Keane, Comparative study of projection schemes for stochastic finite element analysis, Computer Methods in Applied Mechanics and Engineering 195 (19-22) (2006) 2371–2392.

[38] K. Chang, e-Design: Computer-Aided Engineering Design, Academic Press, 2015.

[39] G. S. Szekely, G. I. Schueller, Computational procedure for a fast calculation of eigenvectors and eigenvalues of structures with random properties, Computer Methods in Applied Mechanics and Engineering 191 (8-10) (2001) 799–816.

[40] H. J. Pradlwarter, G. I. Schueller, G. S. Szekely, Random eigenvalue problems for large systems, Computers & Structures 80 (27-30) (2002) 2415–2424.

[41] R. Ghanem, D. Ghosh, Efficient characterization of the random eigenvalue problem in a polynomial chaos decomposition, International Journal for Numerical Methods in Engineering 72 (4) (2007) 486–504.

[42] S. Adhikari, Structural dynamic analysis with generalized damping models : identification, Mechanical Engineering and Solid Mechanics Series, Wiley - ISTE, London, 2014.

[43] R. L. Fox, M. P. Kapoor, Rates of change of eigenvalues and eigenvectors, AIAA Journal 6 (12) (1968) 2426–2429.

[44] R. B. Nelson, Simplified calculation of eigenvector derivatives, Aiaa Journal 14 (9) (1976) 1201–1205.

[45] S. H. Chen, D. T. Song, A. J. Ma, Eigensolution reanalysis of modified structures using perturbations and rayleigh quotients, Communications in Numerical Methods in Engineering 10 (2) (1994) 111–119.

[46] S. H. Chen, X. W. Yang, H. D. Lian, Comparison of several eigenvalue reanalysis methods for modified structures, Structural and Multidisciplinary Optimization 20 (4) (2000) 253–259.

[47] B. Cochelin, N. Damil, M. Potierferry, Asymptotic numerical-methods and pade approximants for nonlinear elastic structures, International Journal for Numerical Methods in Engineering 37 (7) (1994) 1187–1213.

[48] D. Harville, Matrix Algebra From a Statistician's Perspective, Springer, 1997.

[49] D. J. Dawe, Matrix and Finite Element Displacement Analysis of Structures, Oxford University Press, 1984.

[50] M. Clifford, R. Brooks, A. Howe, A. Kennedy, S. McWilliam, P. Shayler, P. Shipway, An Introduction to Mechanical Engineering: Part 1, CRC Press, 2009.

[51] P. D. Spanos, M. Beer, J. Red-Horse, Karhunen-loeve expansion of stochastic processes with a modified exponential covariance kernel, Journal of Engineering Mechanics-Asce 133 (7) (2007) 773–779.

[52] A. Appleton, Thermodynamic & Mechanical Properties of Matter, Alan Appleton, 1996.

[53] J. Reddy, An Introduction to the Finite Element Method Third Edition, Mcgraw Hill Series in Mechanical Engineering, McGraw-Hill Education, 2005.

[54] J. Reddy, Theory and Analysis of Elastic Plates and Shells, Second Edition, CRC Press, 2006.